2nd International Conference on the Material Point Method for Modelling Soil-Water-Structure Interaction

Anura3D
MPM Research Community

Paper number: mpm2019.52
www.anura3d.com
www.mpm2019.eu

Coupled modeling of bank erosion in the Upper Jingjiang Reach, China

Shanshan Deng[1], Junqiang Xia[1]*, Meirong Zhou[1], Jie Li[1] , Yonghui Zhu[2]
1. State Key Laboratory of Water Resources and Hydropower Engineering Science, Wuhan University, Wuhan 430072, China
2. Changjiang River Scientific Research Institute, Wuhan 430010, China
*Corresponding author. Email: xiajq@whu.edu.cn

ABSTRACT

A coupled model of bank erosion was proposed, integrating the module of bank-toe deformation with the modules of groundwater level change and bank stability analysis. Model validation and multiple tests were conducted. Results show that: (i) a more rapid drawdown of river stage resulted in a more significantly delayed response of groundwater level, indicating that the bank may suffer a higher pore water pressure at the same river stage during the rapid drawdown period; .and (ii) a larger bank erosion volume was predicted, with the delayed response of ground water level being considered.

KEY WORDS: bank retreat; fluvial erosion; groundwater level; coupled model; Upper Jingjiang Reach

INTRODUCTION

Bank retreat is a key component of channel evolution in alluvial rivers, and may leads to serious problems for channel stability, navigation and flood control management and resulting in damage to riparian hydraulic structures (Hooke, 1979; Chen and Duan, 2006; Henshaw et al., 2013; Xia et al., 2014). Better understanding of bank retreat processes is necessary in the contexts of fluvial geomorphology and river engineering (Hooke, 1979; Julian and Torres, 2006; Darby et al., 2007). Although various factors influencing bank retreat have been recognized, the major controls remain unclear and are case-dependent in different rivers (Simon et al., 2000; Julian and Torres, 2006; Xia et al., 2014).

Bank retreat processes can be simulated using both empirical methods and numerical models. Empirical formulae are always developed from field measurements and various regression analyses, which usually correlate the bank erosion rate with some key influencing factors, such as water discharge, soil composition and the number of freeze-thaw events (Julian and Torres, 2006; Pizzuto, 2009; Henshaw et al., 2013). However, these methods lack a mechanic characterization and a detailed description of bank retreat processes. Numerical models can be performed at both section- and reach-scales. The dynamic processes of bank retreat can be simulated at reach-scale, through coupling the module of bank stability analysis with the one-dimensional (1D) or two-dimensional (2D) hydrodynamic and bed evolution modules (Darby et al., 2002; Chen and Duan, 2006; Langendoen and Alonso, 2008; Jia et al., 2010; Lai et al., 2015). Whereas these models are usually time-consuming and require detailed measurements, including elaborate channel topography, bed material composition and bank soil properties of a study reach. Therefore, section-scale models are also widely used for their simplicity and convenience to investigate influencing factors of bank erosion (Darby et al., 2007; Parker et al., 2008; Konsoer et al., 2015; Daly et al., 2015). The Bank Stability and Toe Erosion Model (BSTEM) is commonly adopted to simulate bank retreat processes or to determine key influencing factors (Parker et al., 2008; Midgley et al., 2012; Daly et al., 2015; Konsoer et al., 2016). However, the BSTEM cannot account for the effect of groundwater level change, which has already proven to be an important factor to influence soil properties and stability degrees of cohesive banks (Chiang et al., 2011).

Since the TGP operation, the UJR has suffered continuous channel degradation in the whole reach, and sever bank erosion in local regions. A coupled numerical model at section-scale was thus proposed, integrating the bank-toe deformation module with the modules of groundwater level change and bank stability analysis. Through numerical tests, the effects were illustrated of river stage drawdown rate on groundwater flow, along with the impacts of soil properties on bank erosion simulations.

FRAMEWORK OF A COUPLED MODEL

A section-scale model of bank retreat has been developed, with the simulations of three different processes being coupled, including bank-toe deformation, groundwater flow, and bank stability variation.

Bank-Toe Deformation

Near-bank hydrodynamic processes lead to channel deformation at bank-toe, covering lateral basal erosion and near-bank bed deformation. The former usually causes a steeper bank slope, while the latter may leads to bank heightening. Both of these cases would decrease the degree of bank stability, becoming the primary contributors to mass wasting.

Calculation of Lateral Basal Erosion

The rate of lateral basal erosion is usually expressed by an empirical function of the excess flow shear stress (Hanson and Simon, 2001; Darby et al., 2007). Thus, the lateral erosion width, ΔB (m), during a given period Δt (s), can be calculated by:

$$\Delta B = k_d (\tau_f - \tau_c)^a \Delta t \tag{1}$$

where k_d is the erodibility coefficient in $m^3/(N \cdot s)$, calculated by $k_d = 2.0 \times 10^{-7} \times \tau_c^{-0.5}$ (Hanson and Simon, 2001); a is an empirically derived exponent, generally assumed to be 1.0; τ_c is the critical shear stress of bank soil (N/m^2); and τ_f is the flow shear stress (N/m^2), estimated by $\tau_f = \gamma_f R J$, where γ_f is the unit weight of water (9.81 kN/m^3); R is the hydraulic radius (m), approximated by the water depth; and J is the longitudinal water surface slope.

Calculation of Near-Bank Bed Evolution

The transport of bed load can be neglected in the Jingjiang Reach, which just accounts for less than 4% of the suspended sediment amount (CWRC, 2015; Xia et al., 2016). Bed evolution rate, due to the non-equilibrium transport of suspended load, can thus be determined by (Xia et al., 2013):

$$\rho' \frac{\partial Z_b}{\partial t} = \sum_{k=1}^{M} \alpha_{sk} \omega_{sk} (S_k - S_{*k}) \tag{2}$$

where Z_b is the bed elevation (m); ρ' is the dry density of bed material (kg/m^3); M is the number of the fractions used to represent the gradation of non-uniform sediment; S_k is the suspended sediment concentration for the k^{th} fraction (kg/m^3); S_{*k} is the fractional sediment transport capacity (kg/m^3); α_{sk} is the coefficient of saturation recovery; and ω_{sk} is the effective sediment settling velocity (m/s)

Groundwater Level Variation

Although the river bank in the UJR has a two-layer structure, its cohesive upper layer is so thick that the variation in groundwater level would play a key role in the occurrence of bank failure in this reach. In addition, the non-cohesive lower layer is always submerged, with the top usually below the lowest water level. An unsteady one-dimensional governing equation is therefore adopted herein to describe the groundwater movement with a varying free water surface. The change in groundwater level is usually influenced by dynamic hydrological variables, including rainfall, evaporation and river stage (Z_c) (Darby et al., 2007). The governing equation for the groundwater movement can be written as (Chiang et al., 2011):

$$\mu \frac{\partial Z_g}{\partial t} = k_c \frac{\partial}{\partial y} \left(Z_g \frac{\partial Z_g}{\partial y} \right) + q \tag{3}$$

where Z_g is the groundwater level (m); k_c is the hydraulic conductivity (m/s); μ is the specific yield, estimated by $\mu = 0.117\sqrt[7]{k_c}$ (Xia and Zong, 2015); q is the recharge rate from infiltration (m/s); t is the time (s); and y is the spatial coordinate (m).

Bank Stability Analysis

The method proposed by Osman and Thorne (1988) is adopted and improved to calculate the degree of bank stability, with the effects being included of hydrostatic confining force, pore water pressure and matrix suction. Bank failure events can be further divided into an initial failure and subsequent parallel failures (Osman and Thorne, 1988). In addition, the potential failure plane is assumed to pass through the bank-toe, with the presence of a tension crack at the bank-top.

The safety factor of bank stability (F_s) for planar failure is defined as the ratio of resisting force (F_R) to driving force (F_D):

$$F_S = F_R / F_D \tag{4}$$

Bank failure would occur if F_s is less than a critical value (1.0). F_D in Eq. (7) is given by:

$$F_D = G\sin\beta + P_V\cos\beta - P\sin\theta \tag{5}$$

where G is the unit-length weight of the potential failure block (kN/m); P_V is the pore water pressure on the tension crack (kN/m); P is the hydrostatic confining force (kN/m); and θ is the angle between the direction of P and the normal direction of failure surface (°). F_R is calculated by:

$$F_R = c'L + S\tan\phi^b + (N_p - U_l)\tan\phi' \tag{6}$$

where c' is the effective cohesion (kN/m^2); ϕ' is the effective friction angle (°); L is the length of failure surface (m), and $L = (H_1\text{-}H_t)/\sin\beta$; $\tan\phi^b$ represents the rate of increase in shear strength relative to the matric suction; S is the total matric suction (kN/m) acting on the unsaturated portion of the failure plane; N_p is the total pressure on the failure plane (kN/m), and $N_p = G\cos\beta + P\cos\theta$; U_l is the total uplift force (kN/m), with $U_l = P_U + P_V\sin\beta$, where P_U is the pore water pressure on the saturated portion of the failure plane (kN/m).

MODEL VALIDATION

The proposed model was herein set up to simulate bank erosion processes at four typical sections in the UJR during six hydrological years. The model was validated through comparing the calculations with the measurements, in terms of bank profile and bank erosion volume.

Data Sources and Model Setup

A hydrological year in the Jingjiang reach is conventionally defined as the period from the beginning of October in a year to that in the next year, with field surveys of cross-sectional profiles being usually conducted in October. In this study, repeatedly surveyed cross-sectional profiles were obtained from the Changjiang Water Resources Commission (CWRC), along with the hydrological data during the period 2005-2010, and the corresponding bed material composition. Four typical sections of Jing34, Jing35, Jing55 and Jing60 (Fig. 1), with obvious processes of bank erosion, were selected as the study subjects to conduct model validation. Stage hydrographs at these sections were interpolated from the measurements at the hydrometric station of Shashi and the water gauge stations of Chenjiawan and Haoxue (Fig. 1), with the water surface slopes between these stations being used directly. In addition, bank soil properties at these sections were obtained from the indoor geotechnical tests conducted by Xia and Zong (2015).

Figure 1 Sketch maps of Jingjiang Reach

Bank Erosion Volume

The measured bank erosion volume was herein obtained on the basis of the annually surveyed cross-sectional profiles. Fig. 2 show comparisons between the calculated and measured bank erosion volumes (above the bank-toe) at four typical sections during the period 2005-2010, with the corresponding absolute error (AE=the difference between the calculated volume and the measured volume) and relative error (RE=AE/measured volume) being presented in Table 2. As shown in Fig. 2, the calculated erosion volume generally agrees well with the measured volume. The RE of six-year averaged erosion volume in 2005-2010 ranged from -16.5% to 42.1% at these four sections (negative value meaning an underestimation). The best agreement occurred at Jing34, with the RE being less than 27.5 % except for that in 2007. The value of RE at Jing60 ranged from -43.2% to 46.4%. The worst case occurred at the section of Jing55, with the RE being respectively 575.2% and 1241.6% in the years of 2008 and 2010. During these years, the measured bank erosion volumes were close to zero at Jing55, which hence induced a high RE. The severest bank erosion occurred at Jing35, with the measured maximum and minimum erosion volumes being respectively 393.0 and 160.8 m^3/m. The bank erosion volume at Jing35 was overestimated by 22.7% to 82.2% during 2005—2008, except for the year of 2007 with the RE of 115.2%. However, it was underestimated it by 33.5% to 45.9% in 2009—2010.

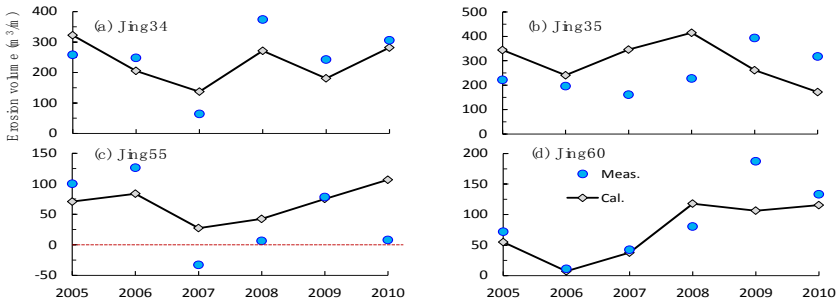

Figure 2 Comparisons between the calculated and measured volumes of bank erosion above the bank-toe at different sections of: (a) Jing34; (b) Jing35; (c) Jing55; (d) Jing60

Bank Stability and Groundwater Level Change

Figs. 3a and 3b show the temporal changes in the safety factor of bank stability (F_s) and the average groundwater level (AGL), respectively at Jing35 in 2009 and at Jing55 in 2006. As indicated in Fig. 3a, four bank failure events occurred in total at Jing35 in 2009, with a high occurrence frequency (3/4) during the flood and recession periods. The time interval between two consecutive failure events was smallest during the flood period (Fig. 3a), due mainly to the intensive fluvial erosion. There were only two bank failure events at Jing55 occurring in the rising and recession periods (Fig. 3b). In addition, it can be found that the groundwater level was obviously delayed as compared with the river stage, especially at Jing55 with a lower soil permeability (Fig. 3b). This delayed response caused the groundwater level to be higher than the river stage during the recession period, and thus induced a higher pore water pressure relative to the hydrostatic confining force, which was unfavorable to bank stability. For example, the groundwater level was on average 2.31 m higher than the river stage at Jing35 in Oct. 2009. However, the difference was just 0.21 m at Jing55 in Oct. 2006, because the bank soil at this section had a lower permeability, resulting in a lower rising rate of groundwater level during the rising and flood periods, and thus leading to a lower groundwater level during recession period.

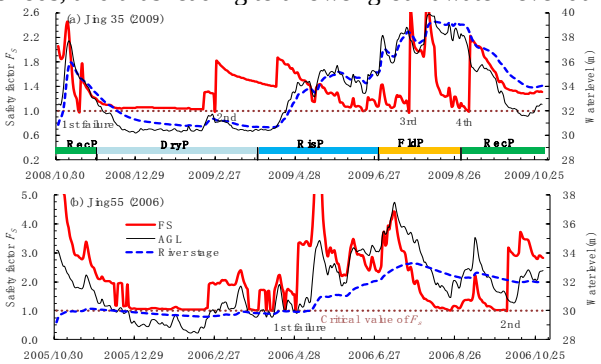

Figure 3 Temporal changes in the safety factor of bank stability (F_s) and the average groundwater level (AGL): (a) at Jing35 in 2009 and (b) at Jing55 in 2006. RecP and DryP are respectively abbreviations of recession period and dry period, with RisP and FldP being respectively rising period and flood period.

DISCUSSION

Multiple tests were conducted to investigate the model behavior, with the effects of river stage drawdown rate and soil permeability on groundwater flow being demonstrated.

Effect of River Stage Drawdown Rate on Groundwater Flow

The bank profile at section of Jing35, measured in Oct. 2008, was used herein as the initial topography, with the average drawdown rate during the period of Sep. to Oct. 2009 being set as the baseline drawdown rate (V_{r0}=0.085 m/d). Five different drawdown rates of rive stage were respectively adopted in cases of R1-R5, at which the river stage decreased from 38.13 m to 33.18 m. The initial ground water level was set to 38.13 m in each case. The drawdown rates (V_r) were respectively 2.0, 1.5 and 1.0 times V_{r0} in cases of R1-R3, and 0.5 and 0.25 times V_{r0} in R4-R5. Bank erosion was not included in these cases in order to merely consider the effect of the drawdown rate of river stage on groundwater flow.

Fig. 4a shows the groundwater tables at the same river stage of 33.18 m in cases of R1-R5. It can be found that a larger drawdown rate of river stage led to a more significantly delayed response of groundwater table, with a higher table being obtained at the same river stage. Fig. 7b shows the relationship between the value of R_V (=V_g/V_r, where V_g is the decrease rate of AGL) and the ratio of V_r to V_{r0}. As indicated in Fig. 4b, there was approximately a negative

exponential relationship between R_v and V_r/V_{r0}, with a correlation coefficient R^2 of 0.99. With an increase in the drawdown rate (a larger V_r/V_{r0}), the value of R_V was decreased, indicating a more obvious decoupling process of groundwater level from the river stage. For example, the values of R_V were respectively 0.84, 0.66 and 0.56 in R5, R3 and R1, where the values of V_r/V_{r0} were respectively 0.25, 1.0 and 2.0. These results indicate that during a more rapid decrease of river stage, there would be a relatively higher groundwater level and thus a higher pore water pressure acting on the bank slope at the same river stage, which is unfavorable to bank stability.

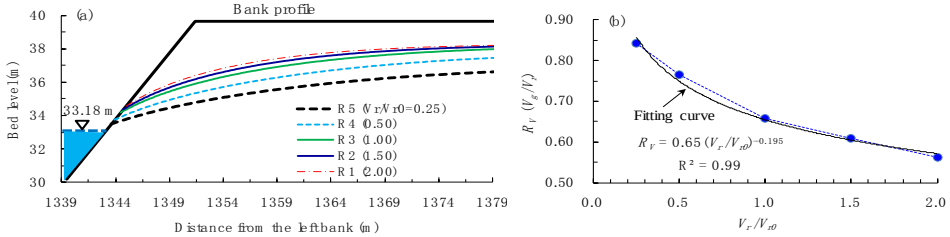

Figure 4. Influence of the drawn rate of river stage on groundwater flow: (a) groundwater tables in cases of R1-R5; and (b) relationship between R_V and V_r/V_{r0}.

Effect of Groundwater Flow on Bank Erosion

Three modes of response of groundwater level to river stage change were applied to investigate the influence of groundwater level change on bank erosion. In the 'delayed response' simulation, the groundwater level was calculated by Eq. (3). In the 'instant response' simulation, the groundwater level was assumed to equal the river stage, and it was assumed to be fixed at the lowest river stage in the 'no response' simulation.

Fig. 5 shows the calculated bank erosion volumes at different sections, using the aforementioned three response modes of groundwater level. As indicated in Fig. 9, the largest and smallest bank erosion volumes were obtained respectively in the first and third response modes in general. The influence of groundwater level was more significant when encountered with severer bank erosion or more mass failure events. The biggest difference between the calculated results of these simulations occurred at Jing35. The average bank erosion volume at Jing35 during the period 2005-2010 was 226.1 m^3/m in the 'instant response' simulation, accounting for 76.3% of that in the 'delayed response' simulation, while the average volume in the 'no response' simulation just accounted for 65.8%. In 2005-2007, the bank erosion volume at Jing60 was not affected by the response of ground water level. This is because the groundwater level can only influence mass failure events instead of fluvial erosion in this study. The bank erosion volume at Jing60 was completely contributed by fluvial erosion in these three years, without the occurrence of mass failure events. Note that with the exception of the influence on the bank erosion volume, the different responses of groundwater level also caused changes in the timing and number of bank failures.

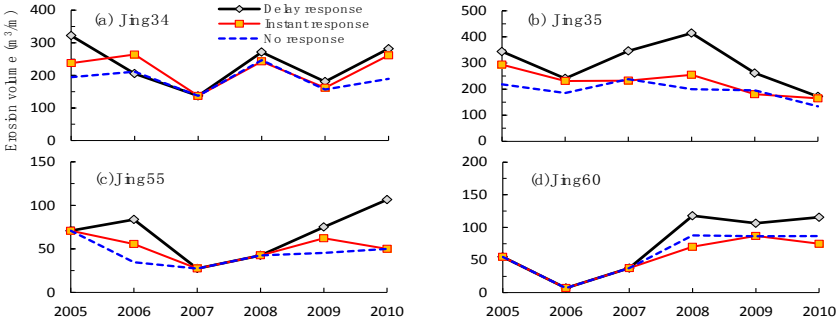

Figure 5 Calculated bank erosion volumes with three types of response of groundwater level to river stage change at different sections of: (a) Jing34; (b) Jing35; (c) Jing55; (d) Jing60.

CONCLUSIONS

A coupled model was proposed for bank retreat processes in the Upper Jingjiang Reach, covering the simulations of bank-toe deformation, groundwater level change and bank stability variation. Model validation and multiple tests were conducted. Following conclusions can be drawn from this study:

(i) There was a relatively higher occurrence frequency of bank failure during the flood and recession periods, due mainly to the intensive fluvial erosion. The groundwater level development was obviously delayed as compared with the river stage, causing a higher pore water pressure relative to the hydrostatic confining force during the recession period, which reduced the degree of bank stability.

(ii) With an increase in the drawdown rate of river stage, the delayed response of groundwater table to river stage change became more significant, with a lower ratio being obtained of the decrease rate of ground water level to the drawdown rate of river stage, and a higher groundwater table at the same river stage being identified. When considering

the delayed response of groundwater level, a larger bank erosion volume was generally obtained, as compared with the cases of 'instant response' and 'no response'.

REFERENCES

Chen D, Duan JG. 2006. Modeling width adjustment in meandering channels. Journal of Hydrology 321 (1): 59-76. Doi: org/10.1016/j.jhydrol.2005.07.034

Chiang S, Tsai T, Yang J. 2011. Conjunction effect of stream water level and groundwater flow for riverbank stability analysis. Environmental Earth Sciences 62 (4): 707–715. Doi: org/10.1007/s12665-010-0557-8

Darby SE, Thorne CR. 1996. Development and testing of riverbank-stability analysis. Journal of Hydraulic Engineering 122 (8): 443–454. Doi: org/10.1061/(ASCE)0733-9429(1996)122:8(443)

Darby SE, Alabyan AM, De Wiel MJ. 2002. Numerical simulation of bank erosion and channel migration in meandering rivers. Water Resources Research 38 (9): (2-1)-(2-12). Doi: 10.1029/2001WR000602

Darby SE, Rinaldi M, Dapporto S. 2007. Coupled simulations of fluvial erosion and mass wasting for cohesive river banks. Journal of Geophysical Research 112 (F3): 1-15. Doi: 10.1029/2006JF000722

Daly ER, Miller RB, Fox GA. 2015. Modeling streambank erosion and failure along protected and unprotected composite streambanks. Advances in Water Resources 81: 114-127. Doi: org/10.1016/j.advwatres.2015.01.004

Hanson GJ, Simon A. 2001. Erodibility of cohesive streambeds in the loess area of the Midwestern USA. Hydrological Processes 15 (1): 23-38. Doi:10.1002/hyp.149

Henshaw AJ, Thorne CR, Clifford NR. 2013. Identifying causes and controls of river bank erosion in a British upland catchment. Catena 100: 107-119. Doi: org/10.1016/j.catena.2012.07.015

Hooke JM. 1979. An analysis of the processes of river bank erosion. Journal of Hydrology 42 (1-2): 39-62. Doi: 10.1016/0022-1694(79)90005-2

Hydrology Bureau of the Changjiang Water Resources Commission (CWRC). 2015. Analysis of channel degradation downstream of the Three Gorges Dam in 2014. Scientific Report of CWRC: Wuhan. (in Chinese)

Julian JP, Torres R. 2006. Hydraulic erosion of cohesive riverbanks. Geomorphology 76 (1): 193-206. Doi: 10.1016/j.geomorph.2005.11.003

Jia DD, Shao X J, Wang H, Zhou G. 2010. Three-dimensional modeling of bank erosion and morphological changes in the Shishou bend of the middle Yangtze River. Advances in Water Resources 33 (3): 348-360. Doi: org/10.1016/j.advwatres.2010.01.002

Konsoer KM, Rhoads BL, Langendoen EJ, Best JL, Ursic ME, Abad JD, Garcia MH. 2016. Spatial variability in bank resistance to erosion on a large meandering, mixed bedrock-alluvial river. Geomorphology 252: 80-97. Doi: org/10.1016/j.geomorph.2015.08.002

Langendoen EJ, Alonso CV. 2008. Modeling the Evolution of Incised Streams: I. Model Formulation and Validation of Flow and Streambed Evolution Components. Journal of Hydraulic Engineering 134 (6): 749-762. Doi: 10.1061/(ASCE)0733-9429(2008)134:6(749)

Lai YG, Thomas RE, Ozeren Y, Simon A, Greimann BP, Wu K. 2015. Modeling of multilayer cohesive bank erosion with a coupled bank stability and mobile-bed model. Geomorphology 243: 116-129. Doi: org/10.1016/j.geomorph.2014.07.017

Midgley TL, Fox GA, Heeren DM. 2012. Evaluation of the bank stability and toe erosion model (BSTEM) for predicting lateral retreat on composite streambanks. Geomorphology 145-146: 107-114. Doi: 10.1016/j.geomorph.2011.12.044

Osman AM, Thorne CR. 1988. Riverbank stability analysis. I: Theory. Journal of Hydraulic Engineering 114 (2): 134-150. Doi: 10.1061/(ASCE)0733-9429(1988)114:2(134)

Parker C, Simon A, Thorne CR. 2008. The effects of variability in bank material properties on riverbank stability: Goodwin Creek, Mississippi. Geomorphology 101 (4): 533-543. Doi: org/10.1016/j.geomorph.2008.02.007

Pizzuto J. 2009. An empirical model of event scale cohesive bank profile evolution. Earth surface process and landforms 34 (9): 1234-1244. Doi: 10.1002/esp.1808

Simon AH, Curini A, Darby SE. Langendoen, E.J., 2000. Bank and near-bank processes in an incised channel. Geomorphology 35 (3): 193-217. Doi: 10.1016/S0169-555X(00)00036-2

Simon A, Pollen N, Langendoen E J. 2006. Influence of two woody riparian species on critical conditions for streambank stability: Upper Truckee River, California. Journal of The American Water Resources Association, 42 (1): 99-113. Doi: 10.1111/j.1752-1688.2006.tb03826.x

Xia JQ, Wang ZB, Wang Y, Yu X. 2013. Comparison of Morphodynamic Models for the Lower Yellow River. Journal of The American Water Resources Association 49 (1): 114-131. Doi: 10.1111/jawr.12002

Xia JQ, Zong QL, Deng SS, Xu QX, Lu JY. 2014. Seasonal variations in composite riverbank stability in the Lower Jingjiang Reach, China. Journal of Hydrology 519: 3664-3673. Doi: org/10.1016/j.jhydrol.2014.10.061

Xia JQ, Zong QL. 2015. Mechanisms and numerical modelling of bank erosion in the Jingjiang Reach of the Middle Yangtze River. Science Press: Beijing. (in Chinese)

Xia JQ, Deng SS, Lu JY, Xu QX, Zong QL, Tan GM. 2016. Dynamic channel adjustments in the Jingjiang Reach of the Middle Yangtze River. Scientific Reports 6(1): 22802. Doi: 10.1038/srep22802